Food Chemistry 405 (2023) 134990

Contents lists available at ScienceDirect

Food Chemistry

journal homepage: www.elsevier.com/locate/foodchem

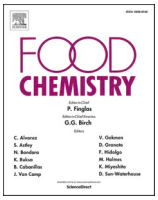

Using rice straw fractions to develop reinforced, active PLA-starch bilayers for meat preservation

Pedro A.V. Freitas *, Consuelo González-Martínez, Amparo Chiralt

Institute of Food Engineering for Development, Universitat Politècnica de València, 46022 Valencia, Spain

ARTICLE INFO

Keywords:
Active food packaging
Phenolic compounds
Antioxidant activity
Cellulose fibres
Rice straw valorisation
Meat shelf life

ABSTRACT

Bilayers from thermoplastic corn starch (TPS) and PLA were obtained, incorporating or not rice straw (RS) valorised fractions: active extract (es) into PLA and cellulose fibres (cf) into TPS films. The films were obtained by thermoprocessing while the bilayers were obtained by thermocompression of the different monolayers (TPS-PLA, TPScf-PLA, TPS-PLAes and TPScf-PLAes). TPS conferred oxygen barrier capacity to the laminates, which was improved by the cf incorporation. The extract slightly reduced the PLA resistance but improved their oxygen barrier capacity. The tensile and barrier properties of the bilayers revealed changes in the performance of each layer associated with the interlayer compound migration. The TPScf-PLAes bags exhibited noticeable antioxidant capacity when used in meat packaging and reduced microbial counts throughout cold storage. Therefore, these bilayers have considerable potential to extend the shelf-life of meat samples, preserving their quality and safety for longer, while using RS fractions permits its valorisation.

1. Introduction

Foods are highly susceptible to processing and storage conditions which directly affect their quality and safety. Each year, it is estimated that microbiological spoilage and oxidative reactions are responsible for >25 % of food losses (Baghi, Gharsallaoui, Dumas, & Ghnimi, 2022; Chawla, Sivakumar, & Kaur, 2021). In this sense, food packaging plays an essential role in maintaining integrity, quality, and food safety, as well as in extending the shelf-life of food during the distribution chain and storage (Topuz & Uyar, 2020). Beyond the traditional purposes, such as cost-effective food protection, with an adequate barrier capacity for oxygen and water vapour, the packaging industries are currently focusing on the development of packaging materials using an environmentally-friendly approach, from renewable, biodegradable, and/or recyclable sources (Topuz & Uyar, 2020). Likewise, the incorporation of active compounds, such as antioxidants and antimicrobial agents, into these biodegradable materials comprises a new and constant challenge in the field of packaging.

Active food packaging is a well-known technology that incorporates additives into packaging materials to preserve or improve the quality of packaged foods as well as to reduce the risk of contamination and foodborne illness (Baghi et al., 2022). The strategy followed by this kind of packaging is based on the release of the active compounds from the packaging to the headspace or the food surface, thus preserving or improving their shelf life throughout storage. Of the active agents, extracts obtained from lignocellulosic-rich agro-industrial waste represent an interesting alternative to synthetic additives. These extracts are made up of a wide variety of phenolic compounds, exhibiting excellent antioxidant and/or antimicrobial properties.

Rice straw (RS) is an agro-industrial residue obtained after harvesting the rice grain, where large amounts of RS are obtained since 1 kg of rice grain generates approximately 1.5 kg of RS (Peanparkdee & Iwamoto, 2019). RS is a lignocellulosic material composed of approximately 37 % cellulose, 20 % hemicellulose, 20 % lignin and 17 % ash (Freitas, González-Martínez, & Chiralt, 2022). The aqueous extraction of RS permitted the obtaining of phenolic-rich fractions (225–486 mg gallic acid equivalent.100 g^{-1} RS) (Menzel, González-Martínez, Vilaplana, Diretto, & Chiralt, 2020; Freitas, González-Martínez, & Chiralt, 2020) with high antioxidant capacity, and cellulose fibres (Freitas et al., 2022) which are high added-value products, useful for application in different fields, such as the development of more sustainable and effective packaging materials.

Overall, biodegradable materials exhibit worsened functional properties than those of petrochemical plastics and the use of a single polymer does not meet the packaging requirements of many foods. To overcome these drawbacks, both the incorporation of reinforcing agents

* Corresponding author.
E-mail address: pedvidef@doctor.upv.es (P.A.V. Freitas).

https://doi.org/10.1016/j.foodchem.2022.134990
Received 12 September 2022; Received in revised form 7 November 2022; Accepted 15 November 2022
Available online 18 November 2022

and additives from renewable resources into the polymer matrices and the obtaining of biodegradable multilayer systems represent feasible alternatives for developing sustainable packaging materials for food systems (Anukiruthika et al., 2020; Wang et al., 2022). Multilayer systems consists of combinations of two or more layers of materials with complementary properties to act as an effective barrier to environmental conditions that cause food spoilage (Kaiser, Schmid, & Schlummer, 2017). The laminates should be materials with improved functional properties with respect to the individual layers, such as enhanced mechanical properties, good oxygen and water vapour barrier properties, sealability, and machinability (Anukiruthika et al., 2020; Kaiser et al., 2017). Combining hydrophilic biodegradable polymers with hydrophobic ones could provide the laminates with improved functional performance (Wang et al., 2022). In this sense, starch is a semicrystalline biopolymer hydrophilic in nature that gives rise to thermoplastic films with excellent barrier properties to lipids, carbon dioxide, and oxygen, but with high permeability to water vapour and water solubility (Galdeano, Mali, Grossmann, Yamashita, & García, 2009). In contrast, poly (lactic acid) (PLA) is a bio-based, biodegradable polyester, hydrophobic in nature, that has good mechanical properties, water vapour barrier capacity and heat sealability, but exhibits low barrier capacity to oxygen (Avérous, Fringant, & Moro, 2001). Thus, starch and PLA films can be combined to produce laminates with improved functional properties for food applications, in which the PLA layer should be the contact face in the case of moist foods.

The aim of this study was to produce biodegradable bilayer films based on PLA and corn starch incorporating bioactive extract and cellulose fibres obtained from RS. The films were characterised as to their barrier, mechanical and optical properties, as well as to their microstructure and thermal behaviour. Likewise, the effectiveness of this packaging material was validated in a real foodstuff, by evaluating the development of the quality parameters (pH, colour, oxidation, and microbial counts) of packaged fresh pork meat throughout 16 days of cold storage.

2. Material and methods

2.1. Materials

Amorphous PLA 4060D, with an average molecular weight of 106,226 D and density 1.24 g/cm^3 was supplied by Natureworks (U.S. A). Corn starch (27 % amylose) was purchased from Roquette (Roquette Laisa, Spain). Poly (ethylene glycol) (PEG1000) and sodium chlorite were obtained by Sigma-Aldrich (St. Louis, MO, USA). Glycerol, acetic acid, sodium carbonate (Na_2CO_3), di-phosphorus pentoxide (P_2O_5), and magnesium nitrate ($Mg(NO_3)_2$) were supplied by PanReac Quimica S.L. U. (Castellar del Vallés, Spain). Gallic acid, Folin-Ciocalteau reagent (2 N), methanol (>99.9 purity), 2,2-Diphenyl-1-picrylhydrazyl (DPPH), sodium chlorite, 2-thiobarbituric acid (>98 % purity), and 1,1,3,3-tetramethoxypropane were supplied by Sigma-Aldrich (St. Louis, MO, USA). Iodine (99.5 % purity) was purchased from Acros Organics® (Geel, Belgium). For microbiological tests, Violet red bile agar (VRB) was purchased from Scharlab S.L. (Sentmenat, Spain). Buffered peptone water, Trypticasein soy broth (TSB), Man, Rogosaand Sharpe agar (MRS) was supplied by Labkem (Barcelona, Spain).

2.2. Active and cellulosic rice straw fractions

The aqueous active extract and cellulose fibres from rice straw (RS) were obtained and characterised in previous studies (Freitas et al., 2020; Freitas, González-Martínez, & Chiralt, 2022) and used to obtain the packaging films. Specifically, RS (Oryza sativa L.), J. Sendra var., from L'Albufera rice fields (Valencia, Spain), was vacuum dried (0.8 mbar, 50 ± 2 °C, 16 h), ground and sieved (particles of under 0.5 mm), before the extraction process. The aqueous RS extract was obtained by applying a combined ultrasound-reflux heating method, with a RS: distilled water ratio of 1:20 (w/v) (Freitas et al., 2020). The total phenolic content (TPC) of the extract, by the Folin-Ciocalteu method, was 37.1 ± 0.4 mg gallic acid equivalent (GAE) per g of freeze-dried extract while its radical scavenging capacity (evaluated by the 2,2-Diphenyl-1-pikryl-hydrazyl (DPPH) radical scavenging method, Brand-Williams, Cuvelier, & Berset, 1995), expressed as EC_{50} value, was 6.3 ± 0.3 mg freeze-dried extract/mg DPPH (Freitas et al., 2020). The cellulose fibres (CF), obtained from the extraction residue, as reported by Freitas et al. (2022), had chemical composition (NREL/TP-510-42,618 method, Sluiter, 2008) of 66 % cellulose, 16 % hemicellulose, 5 % lignin, and 5 % ashes and major cumulative frequencies of lengths and thicknesses of below 200 μm and 5–15 μm, respectively (Freitas, Arias, Torres-Giner, González-Martínez, & Chiralt, 2021, Freitas, González-Martínez, & Chiralt, 2022).

2.3. The preparation of films

2.3.1. PLA monolayers

Amorphous PLA pellets were first conditioned at P_2O_5 for 2 days to eliminate residual water. PLA active films (PLAes), plasticised with PEG1000 at 8 % wt. (with respect to the polymer mass), were obtained by incorporating the freeze-dried RS extract at 6 % wt. with respect to the polymer mass. The PLA/PEG1000 monolayer films without RS extract were prepared as the control formulation (PLA). The film components were previously mixed in a beaker and then melt-blended using an internal mixer (HAAKETM PolyLabTM QC, Thermo Fisher Scientific, Karlsruhe, Germany) at 160 °C and 50 rpm for 6 min. Thereafter, the solid blend was milled using a gridding machine (IKA, model M20, Germany) and compression-moulded using a hydraulic press (Model LP20, Labtech Engineering, Thailand). The milled pellets (3 g) were put onto Teflon sheets and thermoformed by preheating at 160 °C for 3 min, compression at 100 bars at 160 °C for 3 min, and final cooling to 80 °C.

2.3.2. TPS monolayers

Pre-conditioned starch (in P_2O_5 at 25 °C for 5 days) was first-hand mixed with glycerol, as plasticiser, at 30 % wt. with respect to the polymer mass. The composite blend (TPScf) was obtained by incorporating CF into the control mixture (TPS) at 3 % wt. Then, the dispersion was melt-blended in the internal mixer at 130 °C and at 50 rpm for 10 min. The doughs obtained were milled and pre-conditioned at 25 °C and 53 % RH for one week. Afterwards, the milled pellets (4 g per film) were compression-moulded in the hydraulic press by preheating at 160 °C for 3 min, compression at 30 bars and 160 °C for 2 min, followed by 130 bars and 160 °C for 6 min, and final cooling to 80 °C. The TPS and TPScf films were conditioned at 25 °C and 53 % RH (in a chamber with an oversaturated solution of $Mg(NO_3)_2$) for at least one week before characterisation.

2.3.3. Bilayer assembly of PLA and starch monolayers

Bilayer films were prepared by thermocompression of the PLA or PLAes and TPS or TPScf monolayers. The films were preheated at 120 °C for 2 min, compressed at 10 bars and 120 °C for 3 min, and a final cooling to 70 °C. The bilayers obtained were conditioned at 25 °C and 53 % RH at least one week before characterisation.

2.4. Characterisation of films

2.4.1. Microstructural properties and film thickness

Monolayer and bilayer films were immersed in liquid nitrogen and cryo-fractured to observe their cross-section surface by means of a Field Emission Scanning Electron Microscope (ULTRATM 55, Zeiis, Oxford Instruments, UK). Before the microscopic observation, the samples were platinum coated using an EM MED020 sputter coater (Leica BioSystems, Barcelona, Spain). The micrographs were taken under vacuum and 2.0 kV acceleration voltage.

A digital micrometer (Palmer, model COMECTA, Barcelona,

accuracy of 0.001 mm) was used to measure the thicknesses of the films at ten random film positions.

2.4.2. Equilibrium moisture content and water solubility

The equilibrium moisture content of the films was determined gravimetrically by triplicate. To this end, conditioned films (at 25 °C and 53 % RH for two weeks) of about 3 cm × 3 cm were weighed and dried at 60 °C for 24 h. Afterward, the samples were placed in a dissector at 25 °C with P_2O_5 for two weeks, to ensure dry conditions, and weighed. The moisture content was expressed as the total weight loss of the samples during the drying process with respect to their dry weight.

The water solubility of the films was determined according to Talón et al. (2017). Film samples (3 cm × 3 cm) were previously conditioned in P_2O_5 at 25 °C for two weeks to ensure dry conditions. The results were expressed as g of solubilised film/100 g dry film. The analysis was performed in triplicate.

2.4.3. Optical properties

The optical properties of the films were analysed following the Kubelka-Munk theory of multiple scattering using a spectrocolorimeter (CM-3600d, Minolta Co., Japan) (Freitas et al., 2021). Briefly, the reflection spectra were determined from 400 to 700 nm using white and black backgrounds to determine the internal transmittance (Ti) and the infinite reflectance (R_∞). Then, the film colour coordinates L^* (lightness), a^* (redness-greenness), and b^* (yellowness-blueness) were obtained from the R_∞ spectra, using D65 illuminant and 10° observer. Chroma (C^*) and hue angle (h^*) were obtained from the colour coordinates a^* and b^*. The measurements were taken six times for each sample.

2.4.4. Thermal properties

The thermal behaviour of the films was determined by thermogravimetric analysis (TGA) using a thermogravimetric analyser (TGA 1 Stare System analyser, Mettler-Toledo, Switzerland). Conditioned film samples (P_2O_5 at 25 °C for 2 weeks) were weighed (3–5 mg) in alumina pans and heated from 25 to 700 °C under nitrogen atmosphere (10 mL.min^{-1}) at a heating rate of 10 °C.min^{-1}. For each thermal event, the thermogravimetric curves (TGA) and their derivatives (DTGA) were analysed to obtain the initial degradation temperature (T_{on}), the temperature at the maximum degradation rate (T_p), the final degradation temperature (T_{end}), and the mass loss percentage (Δm). The measurements were taken in duplicate.

Differential scanning calorimetry (DSC) was used to determine the phase transitions of the films using a DSC Stare System analyser (Mettler-Toledo GmbH, Switzerland), operating under nitrogen flow (30 mL.min^{-1}). For the PLA films, aluminium-sealed pans containing film samples (5–7 mg) were heated from −25 to 200 °C at a heating rate of 10 °C.min^{-1}, maintained at 200 °C for 5 min, cooled down to −10 °C at −50 °C.min^{-1}, maintained at −10 °C for 5 min, and heated up again to 200 °C at a heating rate of 10 °C.min^{-1}. The starch films were analysed following the Collazo-Bigliardi, Ortega-Toro, and Chiralt (2019) method. Film samples (5–9 mg) were heated from 25 to 160 °C, cooled to 25 °C, and then heated (second heating step) to 160 °C at a heating rate of 10 °C.min^{-1}. All measurements were taken in duplicate.

2.4.5. Barrier properties

The water vapour permeability (WVP) of the films was determined gravimetrically based on the ASTM E96/E96M (Astm, 2005), following the modification proposed by (McHUGH, Avena-Bustillos, & Krochta, 1993). The film samples were cut (Ø = 3.5 cm), placed and sealed in circular Payne permeability cups (Elcometer SPRL, Hermelle/s Argenteau, Belgium) containing 5 mL of distilled water (100 % RH). Afterward, the cups were put into desiccators at 25 °C and 53 % RH (using Mg$(NO_3)_2$ over-saturated solution), thus maintaining a constant RH gradient of 100–53 % through the films, and weighed periodically (ME36S, Sartorius, ±0.00001 g, Fisher Scientific, Hampton, NH, USA), every 1.5 h for 27 h. The WVP of films, expressed in g.mm.kPa^{-1}h^{-1}.m^{-2}, was determined from the water vapour transmission rate, which was obtained from the slope of the weight loss *vs* time curve at the steady state. The analysis was carried out in triplicate.

The oxygen permeability (OP) of the films was obtained using Ox-Tran equipment (Model 1/50, Mocon, Minneapolis, MN, USA) at 25 °C and 53 % RH, according to ASTM D3985-05 (ASTM, 2010). For this, the oxygen transmission rate through the films (50 cm^2) was determined every 15 min until equilibrium was reached. For each treatment, the measurements were taken in triplicate.

2.4.6. Tensile properties

ASTM D882 (ASTM, 2012) was used to obtain the stress–strain curves of the films and to determine the elastic modulus (EM), tensile strength at break (TS), and elongation at break (E) of the films, using a universal test machine (TA.XTplus model, Stable Micro Systems, Haslemere, England). Conditioned film samples (53 % RH at 25 °C for 2 weeks) were cut (25 mm × 100 mm) and stretched at a crosshead speed of 50 mm.min^{-1} by two grips initially separated by 50 mm. Eight samples for each treatment were evaluated.

2.5. Preservation capacity of the bilayer films

Fresh pork meat was purchased from the local market and fillets were cut into 22 ± 1 g pieces, in an aseptic environment, and packaged in thermo-sealed bags of bilayer films (Fig. 3). To this end, laminates of PLA and CF reinforced starch, selected with and without active extract in the PLA sheet (PLA-TPScf and PLAes-TPScf laminates), were chosen on the basis of their better functional properties. The films were cut to 12 cm × 7 cm and sealed using a vacuum sealer (Vacio Press, Saeco) to obtain bags that were thermo-sealed after the meat sample was placed inside. Samples were packaged in duplicate for the analyses at each time. Likewise, meat samples wrapped in a commercial film were used as a control treatment. The packaged samples were stored at 4 °C for 16 days, and the meat quality parameters were evaluated atfter 0, 3, 7, 13, and 16 days of storage in the samples packaged in the different bags.

2.5.1. pH measurement

The pH of the pork meat was determined as described by (Moreno, Atarés, Chiralt, Cruz-Romero, & Kerry, 2018), by direct immersion of the glass electrode probe (Mettler-Toledo GmbH, Schwerzenbach, Switzerland) into the fillets. For each sample, five measurements were taken.

2.5.2. Colour measurement

The meat colour coordinates L^*, a^*, b^*, $C_{ab}{}^*$, and $h_{ab}{}^*$ were determined with a spectrocolorimeter (CM-3600d, Minolta Co., Japan), using a D65 illuminant and 10° observer. The total colour difference (ΔE^*) of the fillets after each storage time with respect to the initial time was determined according to Equation 1.

$$\Delta E^* = \sqrt{(\Delta L^*)^2 + (\Delta a^*)^2 + (\Delta b^*)^2} \quad (1)$$

Where $\Delta L^* = (L^* - L_0^*)$; $\Delta a^* = (a^* - a_0^*)$; $\Delta b^* = (b^* - b_0^*)$; and L_0^*, a_0^*, and b_0^* are the colour coordinates of the fillets at initial time.

2.5.3. 2-thiobarbituric acid reactive substances (TBARS) assay

The lipid oxidation in the packaged meat was determined by the TBARS assay following the (Siu & Draper, 1978) methodology. Briefly, 10 g of meat was homogenised with 50 mL of distilled water and 50 mL of 10 % trichloroacetic acid and homogenised (ULTRA-TURRAX®, Model T 25 D, IKA®, Germany) for 3 min. The dispersion was then filtered and 8 mL of the filtrate was mixed with 2 mL of 2-thiobarbituric acid (0.06 mol.L^{-1}) and heated at 80 °C for 90 min. Afterward, the mixture was cooled to room temperature, and the absorbance at 532 nm

was recorded. TBARS values were expressed as mg malonaldehyde (MDA) per kg of meat using 1,1,3,3-tetramethoxypropane as standard.

2.5.4. Microbiological analysis

A microbiological analysis of the packaged meat after different storage times was performed to quantify total viable counts (TV), psychrotrophic bacteria (PB), total coliforms (TC), and lactic acid bacteria (LA). Briefly, 10 g of meat sample was aseptically taken, mixed with 90 mL of 0.1 % peptone water in sterile bag, and homogenised using a Masticator paddle blender (IUL Instruments, Barcelona, Spain) for 3 min. The resulting dispersion was serially diluted by transferring 1 mL of each dilution into 9 mL of tryptic soy broth (TSB), thus obtaining a 10^{-2} dilution. From this, serial dilutions were obtained, and 1 mL of each dilution tube was mixed with the appropriate medium to quantify the corresponding microorganism. TC was quantified in the chromogenic medium Brilliance *E. coli*/Coliforms Selective Agar by incubation at 37 °C for 24 h. The LA was determined using MRS agar after incubation at 30 °C for 72 h. Finally, the TV and PB were quantified in PCA plates by incubation at 37 °C or 4 °C for 48 or 7 days, respectively. For each treatment, plates with 25 to 250 colonies were selected to determine the bacterial counts, which were expressed as log colony-forming units per gram of meat (log CFU.g^{-1}).

2.6. Statistical analysis

The experimental data were analysed through an analysis of variance (ANOVA) using the Minitab Statistical Program (version 17) with a confidence level of 95 %. Tukey's studentised range (HSD) test was performed to determine whether there were significant differences between the formulations, using 5 % least significant difference (α).

3. Results and discussion

3.1. Structure and appearance of films

Fig. 1a-d shows the FESEM micrographs of the cross-sections of the different bilayer films made up of thermoplastic starch and PLA with and without CF (in TPS films) or RS extract (in PLA films). Micrographs of the different monolayers at higher magnifications before and after their thermoassembly were also shown in Fig. 1e-l. Both TPS and PLA layers without additive exhibited the typical homogeneous microstructure previously described for glycerol plasticised corn starch (Collazo-Bigliardi et al., 2019) and PEG plasticised amorphous PLA (Muller, González-Martínez, & Chiralt, 2017). The good interfacial compatibility between the starch and PLA monolayers was deduced from the non-delamination or detachment that occurs despite the cryo-fracture mechanical stress, as also reported by other authors (Muller et al., 2017). In the studied laminates, PLA is an amorphous polymer, containing a fraction of low molecular oligomers, which may contribute to the increase in its polarity and chemical affinity with starch molecules at the interface (Muller et al., 2017). Nevertheless, changes in the microstructure of the respective monolayers after the thermoadhesion process (Fig. 1e-l) could be attributed to the interlayer compound migration and the subsequent changes in the compound arrangement in the final bilayer. Thus, low molecular weight compounds, such as water and glycerol, could migrate from the starch layer to PLA and PEG1000 or extract compounds could migrate from the PLA to the starch sheet.

In Fig. 1e-l, the microstructural changes occurring in the PLA layer due to the incorporation of the RS extract before and after the thermosealing step can be observed. The incorporation of the RS extract promoted differences in the cryofracture behaviour, also exhibiting a small proportion of fine dispersed particles in the PLA matrix. This suggests a partial compatibility of the extract compounds with the polymer matrix. Some extract components could be homogeneously integrated into the polymer network, but some others aggregated, forming a finely dispersed phase. Some authors (Menzel et al., 2020; Freitas et al., 2020; Karimi et al., 2014) identified several phenolic compounds in the aqueous RS extracts, such as *p*-coumaric, protocatechuic, ferulic, caffeic and vanillic acids, which could establish hydrogen bonds with the carbonyl group of PLA chains or with the end chain hydroxyls. The presence of miscible and non-miscible compounds within the polymer matrix modified the films cryofracture pattern, which can also affect the physical properties of the films.

The CF particles in TPS films may be clearly appreciated in Fig. 1i-k. The composite structure did not show any cracks or gaps between the CF and TPS matrices, which suggested good interfacial compatibility and entanglement, as observed in previous studies (Freitas et al., 2021). After the thermosealing of the bilayers, CF appeared even better integrated in the starch matrix, thus indicating the promotion of the chemical affinity between the polymer matrix and CF in the bilayers. Likewise, the cryofractured surface of the starch matrix in the bilayers (Fig. 1j-l) revealed changes in the component arrangement which can be attributed to the interlayer component migration.

Table 2 shows the thickness of the different films, where the PLA monolayers were thinner than the TPS monolayers. This agrees with the lower mass (3 g) of the PLA sheets when compared to the TPS (4 g), but also with the slower creep of starch during thermocompression. This flow was reduced even more when CFs were present in the blend, which can be attributed to the glycerol interactions with CF that weakened its plasticising effect (Freitas et al., 2021). As can be inferred from Fig. 1 and Table 2, none of the bilayer films were as thick as those estimated from the sums of the thicknesses of the separated monolayers, which suggests the radial flow of the polymer layers during the thermadhesion step. The reduction was about 12, 18, 15, and 20 % for PLA-TPS, PLA-TPScf, PLAes-TPS, and PLAes-TPScf bilayers, respectively. In every case, the PLA layers showed the greatest thinning, whereas the TPScf was thicker than the TPS layer. Differerences between the thicknesses of the layers can be attributed to the interlayer migration of low molecular compounds (water and glycerol) and the different flowability of the polymer matrices during the thermoadhesion step. These effects were also observed by other authors (Andrade, González-Martínez, & Chiralt, 2022) studying multilayer films based on PLA/poly(vinyl alcohol)/PLA laminates.

The internal transmittance (T_i) of all films and their psychometric colour coordinates (L^*, C_{ab}^*, and h_{ab}^*) are shown in Fig. 2, and Table 1, respectivelly. The neat PLA monolayer exhibited the highest T_i and L^* values, coherent with the higher degree of homogeneity and transparency of the polymer matrix. The incorporation of the RS extract turned the PLAes film a yellowish-brown and made it darker, characterised by the higher values of C_{ab}^* and the lower values of L^* and h_{ab}^*, while the films exhibited a noticeable decrease in the T_i values. This was due to the presence of coloured compounds of the RS extract, which promoted selective light absorption and scattering. However, no significant changes in either the T_i or colour coordinates were observed after the incorporation of CF into the TPScf film. Similar results were found by Fourati, Magnin, Putaux, and Boufi (2020) when analysing starch films reinforced with different cellulosic fractions.

The colour and appearance of the bilayer films were greatly influenced by the corresponding monolayers, as observed in the T_i spectra (Fig. 2) and colour coordinates (Table 1). The bilayer films without the extract (PLA-TPS and PLA-TPScf) exhibited optical properties that were similar to those of starch films, while the bilayers with the RS extract (PLAes-TPS and PLAes-TPScf) were more similar to the PLAes film. Nevertheless, there were differences in the bilayers that could be associated with the structural changes promoted by thermoadhesion, as previously commented on. It was the bilayer assembly of PLAes with TPS or TPScf in particular that promoted internal transmittance with respect to the PLAes monolayer, mainly when CF were not present in the starch layer, and the films exhibited a higher degree of lightness and less colour saturation. Therefore, the starch layer attenuated the colour effects of the RS extract, mainly when it did not contain CF. Likewise, the bilayers of PLA without the RS extract with TPScf were less transparent than the

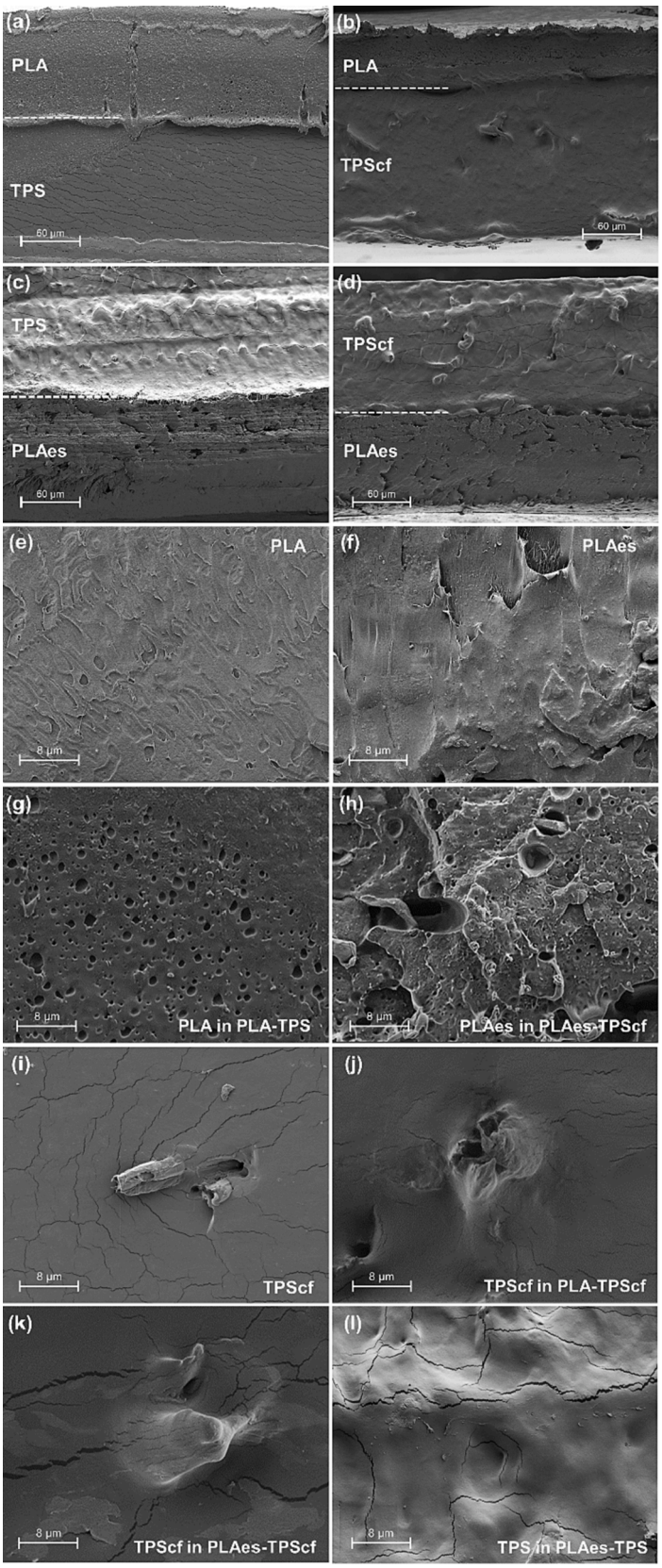

Fig. 1. FESEM images of the cross-section of PLA/starch bilayers (a: PLA-TPS, b: PLA-TPScf, c: PLAes-TPS and d: PLAes-TPScf), showing the interface (dashed line) between sheets, and micrographs at higher magnification of the monolayers before and after thermo-adhesion in the different bilayers (e: PLA: before; f: PLAes before; g: PLA in PLA-TPS; h: PLAes in PLAes-TPScf; i: TPScf: before; j: TPScf in PLA-TPScf; k: TPScf in PLAes-TPScf; l: TPS in PLAes-TPS).

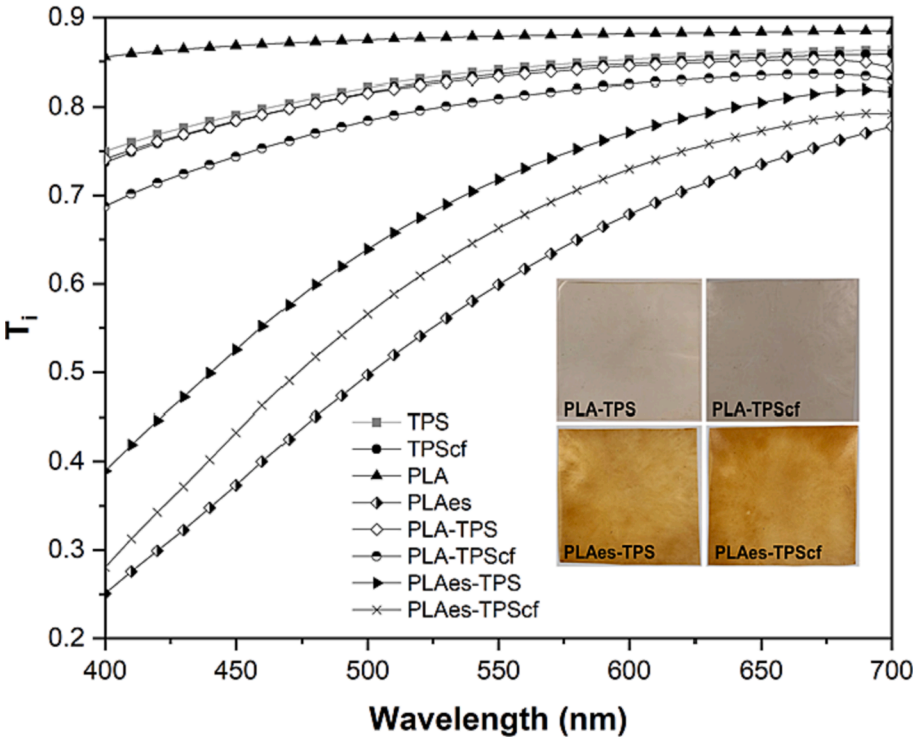

Fig. 2. The internal transmittance (T_i) of the monolayers (TPS, TPScf, PLA, PLAes) and bilayer films (PLA-TPS, PLA-TPScf, PLAes-TPS, and PLAes-TPScf) and the visual appearance of the bilayer films.

TPS, exhibiting a darker and more saturated colour. Therefore, differences in the light interactions in the bilayers affected their colour and transparency that were also affected by the structural changes promoted by thermoadhesion.

3.2. *Water relations and barrier and tensile properties of the films.*

Table 2 gives the equilibrium moisture content and water solubility of the different mono- and bilayers. The incorporation of the RS extract into the PLA matrix or CF into the starch matrix did not affect ($p > 0.05$) the moisture content or the water solubility with respect to their corresponding control monolayer. The hydrophobic PLA matrix had markedly lower water sorption capacity and water solubility than starch films, which makes it desirable for wet food contact applications. As expected, although the bilayers exhibited intermediate equilibrium moisture content values compared to the PLA and starch monolayers, they were higher than what was expected from the mass balance in the bilayer (3:4 mass ratio in PLA:TPS layers). This suggests that the water binding capacity of the PLA increased in the bilayer assembly, probably due to the interlayer migration of water from the starch sheet and the subsequent progress of PLA hydrolysis involved in the thermosealing step. This effect was similar in the four bilayers, suggesting similar changes during the thermosealing step in every case. In contrast, the bilayer water solubility was in the range of that expected from the individual solubility of each layer and its mass fraction in the bilayer.

Table 2 shows the values of WVP, OP, and the tensile properties of the different monolayer and bilayer films. The PLA films exhibited a good water vapour barrier capacity that was slighlty worsened by the RS extract, whereas the starch films exhibited a better oxygen barrier capacity that was enhanced by CF incorporation. The incorporation of RS extract into the PLA monolayer (PLAes) and CF into the starch film (TPScf) provoked a decrease of 7 and 26 %, respectively, in the OP values with respect to their corresponding controls. The presence of hydrophilic components from the extract in the PLA matrix could reduce the solubility of oxygen molecules, while the presence of CF increases the tortuosity factor for the mass transfer of the starch films, thus limiting the diffusion rate of oxygen through the matrix (Freitas et al., 2021). It is worth mentioning that the presence of antioxidant phenolic compounds could promote the oxygen scavenging effect, as an additional oxygen barrier effect of the films.

The bilayers exhibited WVP values similar to those of the PLA monolayers, while the OP values were closer to those of the starch films. This is coherent with the lamination theory, which states that the barrier properties of a multilayer system are closer to those of the monolayer with the highest barrier capacity (Siracusa, 2012). In fact, the theoretical values of OP and WVP determined according to the perpendicular mass transfer model with parallel assembled resistances, were very similar (predicted range of WVP values: 0.20–0.27 g.mm.kPa^{-1}.h^{-1}.m^{-2}, and OP values: 9.0–14.0 cm^3.m^{-1}.s^{-1}.Pa^{-1}) to the experimental values for both WVP and OP. Thus, the WVP of the PLA-TPS and PLA-TPScf bilayers did not differ ($p > 0.05$) from that of the PLA film with or without extract, while the incorporation of the extract into the PLA films led to a slight increase in the WVP values for PLAes-TPS and PLAes-TPScf bilayers. The differences with respect to the theoretical values were greater in the case of WVP than in that of OP, which suggests greater changes in the PLA limiting layer for water transfer during thermoadhesion. The phenolic acids from the RS extract could promote the partial hydrolysis of PLA chains, mainly during thermocompression, which would alter the interchain forces of the polymer network, favouring the diffusion of water vapour through the films.

As concerns the oxygen barrier, the presence of the RS extract (in PLAes-TPS) or CF (in PLA-TPScf) in the bilayers had a similar decreasing effect on the OP values, with respect to the PLA-TPS laminate, (about 41 % and 46 %, respectively) while a non-additive effect was observed for the PLAes-TPScf bilayer.

Therefore, the lamination of PLA and starch films was effective at obtaining bilayer assemblies with an improved water vapour and oxygen barrier capacity, although the improvement was affected by the potential interlayer migration of low molecular compounds. From the point of view of the barrier capacity, the best combination was PLA-

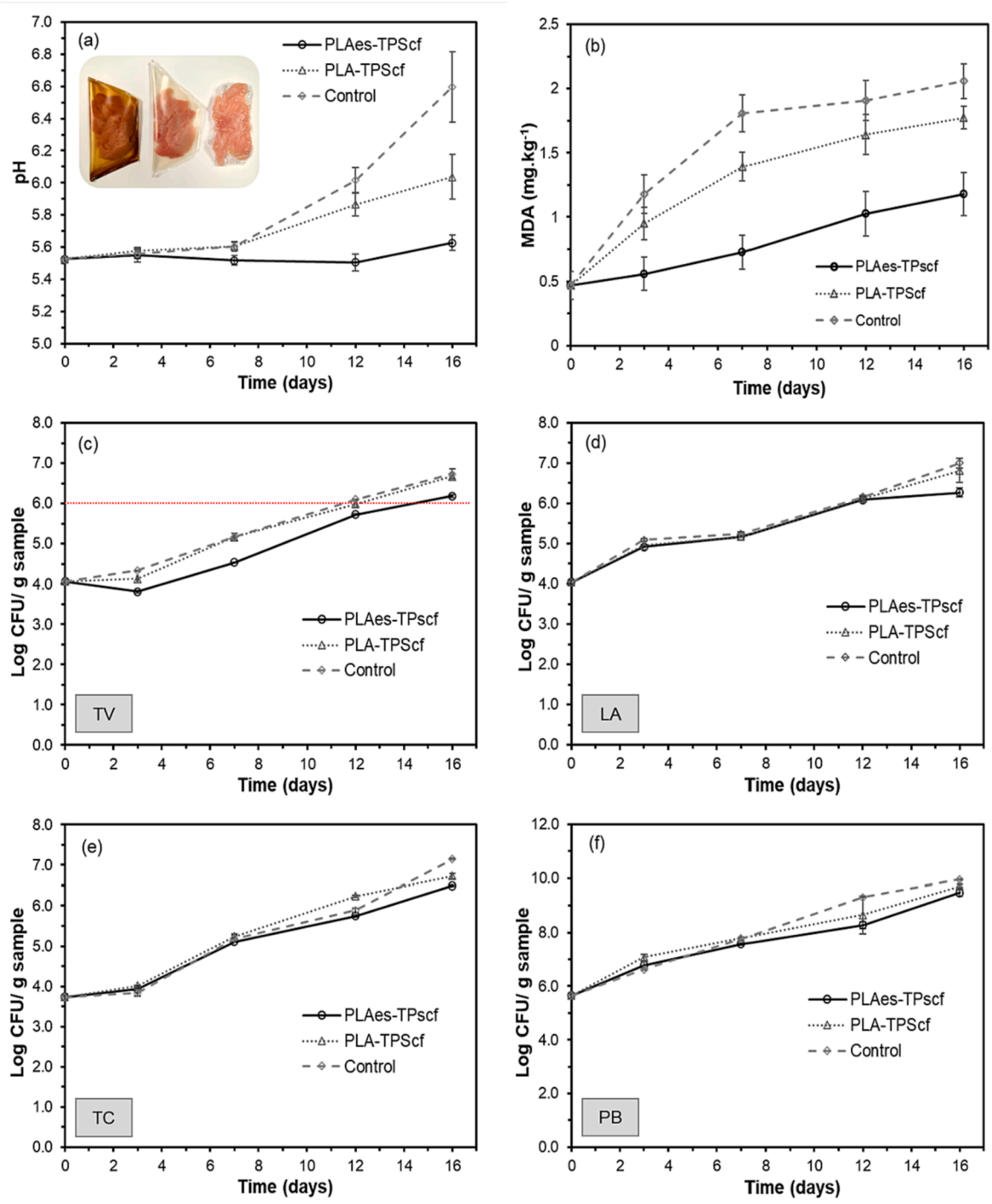

Fig. 3. Development of pH values (a), TBARS index (b), and microbial counts (c, d, e, f) (total viable counts (TV), psychrotrophic bacteria (PB), total coliforms (TC), and lactic acid bacteria (LA)) of pork meat samples packed with bilayer (PLAes-TPScf and PLA-TPScf) thermosealed bags and control sample wrapped with a commercial film, stored at 4 °C for 16 days.

TPScf, although PLAes-TPScf also exhibited the best oxygen barrier capacity.

The PLA and TPS monolayer exhibited values of tensile parameters (Table 2) in the range of previously reported values (Vilarinho et al., 2021; Collazo-Bigliardi et al., 2019; Freitas et al., 2021). The incorporation of the RS extract reduced the TS and E values of the PLA film by about 11 and 46 %, respectively. This implied a weakening effect in the matrix due to the reduction in the inter-chain forces with the newly established molecular interactions with the extract components. In contrast, CF greatly promoted the stiffness and resistance to break of TPS films, as previously reported (Freitas et al., 2021). In general, all bilayers became markedly less resistant and stiff than PLA films, as well as less stretchable than TPS films. These noticeable changes in the tensile properties with respect to what is expected from the PLA monolayer (the most resistant and less extensible) is coherent with the previously mentioned interlayer compound migration that altered the initial properties of the layers. The partial hydrolysis of PLA chains promoted by the water diffusion from TPS could affect the PLA mechanical resistance with the subsequent effect on the bilayer tensile behaviour. Lim et al. (2010) suggest that a moisture content in PLA resin above 250 ppm

Table 1
Colour parameters, lightness (L^*), chroma (C_{ab}^*), and hue angle (h_{ab}^*) of the monolayer and bilayer films. Mean values and standard deviations.

Formulation	L^*	C_{ab}^*	h_{ab}^*
PLA	90.7 ± 0.2^{a}	2.51 ± 0.13^{e}	99.6 ± 0.8^{a}
PLAes	67.6 ± 0.7^{f}	34.57 ± 0.65^{a}	77.1 ± 0.3^{f}
TPS	88.5 ± 0.1^{b}	7.57 ± 0.10^{d}	92.5 ± 0.1^{b}
TPScf	88.1 ± 0.2^{b}	8.25 ± 0.35^{cd}	92.6 ± 0.2^{b}
PLA-TPS	87.3 ± 0.3^{b}	7.58 ± 0.11^{d}	92.2 ± 0.3^{b}
PLA-TPScf	86.0 ± 0.5^{c}	9.50 ± 0.31^{c}	90.9 ± 0.4^{c}
PLAes-TPS	76.9 ± 1.2^{d}	27.92 ± 2.06^{b}	83.4 ± 0.7^{d}
PLAes-TPScf	72.2 ± 0.9^{e}	34.41 ± 1.22^{a}	81.0 ± 0.6^{e}

Different subscript letters in the same column indicate significant differences via the Tukey test ($p < 0.05$).

can lead to severe hydrolytic degradation during the thermal treatment, which provokes a molecular weight drop and alters the functional properties of PLA-based materials. The active bilayers (PLAes-TPS and PLAes-TPScf) were the least resistant to break and least stretchable ($p < 0.05$), which suggests that phenolic acids could also contribute to the partial hydrolysis of the PLA matrix. Muller et al. (2017) also found this effect in PLA/starch bilayer films containing cinnamaldehyde. Although the incorporation of CF into the starch film increased the TS and EM values by approximately 100 % and 300 %, respectively, this reinforcing effect was not observed ($p < 0.05$) in the corresponding bilayers (PLA-TPScf and PLAes-TPScf) since the properties of the assembled PLA film were of superior strength, thus masking the improvement in the starch film resulting from the incorporation of CF.

3.3. Thermal behaviour of the films

TGA and DSC analyses were performed to evaluate potential changes in the thermal behaviour of polymers associated with the thermoassembly step. Table 3 gathers the thermogravimetric parameters of each thermal degradation event, as well as the glass transition temperature (T_g) of the polymers in the films before and after thermocompression. Except for the PLA and PLAes monolayers, all films exhibited a first thermodegradation step ranging between 35 and 120 °C, corresponding to the loss of bonded water present in the starch matrix.

The neat and active PLA monolayers exhibited a single thermodegradation step, with a Δm of about 97–98 %, as also reported by other

Table 2
Thickness, moisture content, water solubility, water vapour permeability (WVP), oxygen permeability (OP), and tensile properties (E: elongation at break; TS: tensile strength; EM: elastic modulus) of monolayer and bilayer films. Mean values and standard deviations.

Formulation	Experimental thickness (mm)	Moisture (%)	Solubility (g soluble solids/100 g film)	WVP ($g.mm.kPa^{-1}.h^{-1}.m^{-2}$)	OP ($x10^{14}$) ($cm^3.m^{-1}.s^{-1}.Pa^{-1}$)	E (%)	TS (MPa)	EM (MPa)
PLA	0.146 ± 0.008^{c}	0.7 ± 0.1^{c}	1.2 ± 0.4^{c}	0.11 ± 0.01^{e}	165.9 ± 1.1^{a}	6.0 ± 0.7^{e}	34.2 ± 0.5^{a}	1255 ± 36^{a}
PLAes	0.144 ± 0.007^{c}	0.9 ± 0.1^{c}	1.9 ± 0.8^{c}	0.15 ± 0.01^{e}	154.3 ± 5.3^{b}	3.2 ± 0.2^{f}	30.5 ± 1.6^{b}	1315 ± 76^{a}
TPS	0.171 ± 0.026^{bc}	8.3 ± 0.2^{a}	42.4 ± 1.6^{a}	6.32 ± 0.19^{a}	9.0 ± 0.5^{d}	30.4 ± 3.5^{a}	3.4 ± 1.0^{g}	175 ± 53^{c}
TPScf	0.185 ± 0.025^{b}	8.0 ± 0.6^{a}	36.9 ± 4.1^{a}	5.94 ± 0.17^{b}	6.6 ± 0.7^{e}	12.3 ± 5.0^{cd}	6.8 ± 1.2^{f}	551 ± 150^{b}
PLA-TPS	0.278 ± 0.033^{a}	6.9 ± 0.3^{b}	18.3 ± 3.8^{b}	0.42 ± 0.06^{de}	16.8 ± 0.7^{c}	19.4 ± 4.7^{b}	11.7 ± 1.0^{cd}	555 ± 22^{b}
PLA-TPScf	0.273 ± 0.012^{a}	6.7 ± 0.4^{b}	18.3 ± 1.3^{b}	0.24 ± 0.09^{e}	9.4 ± 1.0^{d}	16.1 ± 3.0^{bc}	12.4 ± 1.2^{c}	611 ± 16^{b}
PLAes-TPS	0.269 ± 0.013^{a}	6.7 ± 0.3^{b}	17.9 ± 0.8^{b}	0.87 ± 0.12^{c}	10.3 ± 0.8^{d}	13.7 ± 3.2^{c}	7.82 ± 1.4^{ef}	507 ± 23^{b}
PLAes-TPScf	0.262 ± 0.007^{a}	6.6 ± 0.1^{b}	18.1 ± 0.6^{b}	0.61 ± 0.07^{cd}	9.6 ± 1.2^{d}	8.4 ± 2.5^{de}	9.6 ± 1.0^{de}	574 ± 38^{b}

Different subscript letters in the same column indicate significant differences via the Tukey test ($p < 0.05$).

Table 3
Thermal degradation events, with the onset (T_{on}) and peak (T_p) temperatures, mass loss (Δm) and final residue obtained from the TGA curves, and glass transition temperature (mid-point: T_g) obtained from the second heating scan of DSC, for the PLA and TPS layers before (monolayers) and after (bilayers) thermocompression. Mean values and standard deviations.

Formulation	TGA										DSC	
	[35–120] ℃			[150–460] ℃			[435–665] ℃			Residue	T_{gPLA}	$T_{gStarch}$
	T_{on}	T_p	Δm (%)	T_{on}	T_p	Δm (%)	T_{on}	T_p	Δm (%)			
PLA	–	–	–	190 ± 6^{b}	376 ± 1^{a}	97.3 ± 0.1^{a}	–	–	–	0.4 ± 0.2^{c}	37.7 ± 2.5^{ab}	–
PLAes	–	–	–	234 ± 1^{a}	342 ± 1^{b}	98.5 ± 0.2^{a}	–	–	–	1.1 ± 0.3^{b}	34.2 ± 1.5^{bc}	–
TPS	44 ± 2^{b}	67 ± 2^{a}	1.8 ± 0.1^{b}	156 ± 1^{c}	333 ± 1^{bc}	80.7 ± 1.0^{c}	432 ± 2^{c}	548 ± 3^{e}	16.5 ± 1.2^{a}	0.7 ± 0.2^{c}	–	92.4 ± 4.1^{a}
TPScf	50 ± 2^{a}	65 ± 1^{ab}	1.4 ± 0.5^{b}	152 ± 4^{c}	332 ± 1^{c}	82 ± 1.0^{c}	448 ± 3^{b}	564 ± 2^{c}	15.3 ± 1.5^{a}	1.3 ± 0.1^{b}	–	85.2 ± 6.4^{a}
PLA-TPS	36 ± 1^{c}	58 ± 1c	2.5 ± 0.3^{a}	153 ± 3^{c}	334 ± 2^{bc}	85.3 ± 1.6^{b}	461 ± 2^{a}	589 ± 9^{ab}	10.6 ± 1.1^{b}	2.1 ± 0.6^{a}	37.2 ± 0.6^{ab}	68.8 ± 5.4^{b}
PLA-TPScf	41 ± 2^{b}	64 ± 1^{ab}	1.8 ± 0.3^{ab}	154 ± 8^{c}	335 ± 1^{bc}	87.4 ± 0.5^{b}	462 ± 3^{a}	554 ± 1^{d}	10.2 ± 1.1^{b}	2.3 ± 0.4^{a}	37.8 ± 0.3^{a}	62.2 ± 0.5^{bc}
PLAes-TPS	35 ± 1^{c}	62 ± 2^{b}	1.9 ± 0.2^{ab}	152 ± 1^{c}	338 ± 1^{bc}	83.8 ± 0.5^{bc}	465 ± 1^{a}	600 ± 3^{a}	11.2 ± 2.1^{b}	2.0 ± 0.2^{a}	35.4 ± 0.5^{abc}	66.0 ± 1.5^{bc}
PLAes-TPScf	46 ± 3^{b}	66 ± 6^{ab}	1.1 ± 0.4^{b}	158 ± 3^{c}	338 ± 3^{bc}	84.2 ± 0.4^{bc}	459 ± 1^{a}	566 ± 8^{c}	13.7 ± 0.6^{ab}	2.2 ± 0.4^{a}	31.7 ± 1.0^{c}	58.3 ± 0.5^{c}

Different subscript letters in the same column indicate significant differences via the Tukey test ($p < 0.05$).

authors (Rasheed, Jawaid, Karim, & Abdullah, 2020). The incorporation of RS extract markedly decreased the T_p of the PLA film (from 376 to 342 °C), which also suggests that the extract components weakened the intermolecular forces of the PLA/PEG 1000 matrix, as commented above. Nonetheless, the active PLA films exhibited higher T_{on} than the control PLA, which could be related to the establishment of interactions between the extract's compounds and the polymer matrix, thereby delaying its initial degradation.

The second thermodegradation stage of the bilayers is related to the thermal decomposition of both the starch/glycerol (Kargarzadeh, 2017) and PLA/PEG 1000 (Rasheed, Jawaid, Parveez, Hussain Bhat, & Alamery, 2021) matrices, with and without CF (Freitas et al., 2021) or RS extract. As shown in Fig. S1 and Table 3, the bilayers did not exhibit noticeable differences, showing similar values of T_{on} (152–158 °C), T_p (334–338 °C), and Δm (84–87 %). The PLA-TPS sample exhibited a slightly faster mass change at the beginning of the second thermal event (Fig. S1b) than the other bilayers, which may be due to the molecular interactions, either of the extract compounds or the CF, with the low molecular weight polymer chains, which delayed their thermodegradation to some extent. The active bilayers exhibited a retarded degration at the end of this step, which could be attributed to the contribution of extract components in terms of their own thermodegradation or their interactions with the degradation mechanisms of the polymers.

The third and last stage of degradation (435–665 °C) occurred for the starch monolayers and every bilayer, and corresponds to the degradation of the first step fragmentation products of the starch films (Danilovas, Rutkaite, & Zemaitaitis, 2014). Of the bilayers, the laminates with the RS extract exhibited higher Δm, which could be due to the degradation of the lignin fraction present in the extract.

The T_g values (obtained from the second heating step of the DSC analyses) of all films are shown in Table 3. The T_g for PLA was similar to that previously reported for the polymer plasticised with PEG (Muller et al., 2017), while glycerol-plasticised TPS also exhibited T_g in the previously described range (Collazo-Bigliardi et al., 2019). The presence of the RS extract did not significantly change ($p > 0.05$) the T_g of the PLA matrix, although a decreasing trend was observed, thus indicating a plasticising effect. As deduced from the tensile behaviour, the extract components reduced the interchain forces of the PLA/PEG1000 matrix, resulting in lower strength matrices, as also observed in PLA films when ferulic or cinnamic acids were incorporated (Ordoñez, Atarés, & Chiralt, 2022). The T_g value of starch was not affected by the incorporation of CF, although Avérous et al. (2001) reported an increase in T_g determined by DMA in reinforced TPS matrices with CFs. As concerns the bilayers, submitted to thermocompression, a marked reduction in the T_g values of starch was observed, mainly when CFs were present, which could be attibuted to the interlayer migration of low molecular weight compounds that provoked changes in the layers' composition, thus affecting their initial properties. The incorporation of CF into the starch matrix modifies the water interactions with the components (Avérous et al., 2001), which could promote the migration of the hydrophilic components present in the RS extracts. This would lead to a decrease in the cohesiveness of the starch network, either by weakening the interchain forces or even through the partial hydrolysis of the polymer. Menzel et al. (2020) reported the depolymerisation of amylose by thermal processing, which was reduced by the protective effect of glycerol and enhanced in the presence of RS extracts. Therefore, the migration of glycerol from the starch sheet and RS extract phenolic acids from PLA could lead to amylose depolymerisation during thermocompression and T_g reduction. In contrast, no significant changes in the T_g values of the PLA layers was observed with respect to the corresponding monolayers, except when these contained extract and were in contact with the TPScf layer. The migration of both water and glycerol molecules from the starch to the PLA layer could enhance the effect of the extract within the PLA matrix. These greater changes were also observed in the mechanical behaviour of the bilayer, with a reduction in TS and E.

The thermal behaviour also confirmed the migration of low MW compounds between layers during their thermoadhesion, which modified the initial properties of the monolayers. However, even accounting for this effect, the bilayers exhibited global properties that better meet food packaging requirements in terms of their water vapour and oxygen barrier capacity, maintaining mechanical resistance and flexibility, and, with potential antioxidant and antibacterial capacity, in the case of active laminates.

3.4. Pork meat preservation with bilayer bags.

The obtained bilayers, both CF-reinforced and with and without RS extract, were used to evaluate their capacity to preserve fresh pork meat. Fig. 3 shows the changes in the different quality parameters of fresh pork meat packaged with the PLA-TPScf and PLAes-TPScf bilayers, as compared with samples wrapped in a commercial film, throughout 16 days of cold storage (4 °C).

The pH is an important indicator of meat quality since it affects its water retention capacity, colour, and flavour (Kim, Jeong, Seol, Seong, & Ham, 2016). As shown in Fig. 3a, the initial pH value of the meat was 5.5, in line with values found for fresh pork meat (Yang, Xie, Jin, Liu, & Zhang, 2019). The storage time and the type of packaging significantly affected the pH values of the samples ($p < 0.05$). Overall, the meat exhibited an increase in pH values throughout storage, which is characteristic of the enzymatic and/or microbiological deterioration of proteins that give rise to alkaline substances, such as amines (Pacquit et al., 2006). Although statistically different over time, the samples packed with the PLAes-TPScf bilayer did not exhibit a marked increase in pH (5.5 to 5.6), suggesting that the active film was more efficient than the other treatments at maintaining the pH of the meat. Furthermore, as compared with the control sample, the PLA-TPScf control bilayer was more efficient at maintaining the pH of the sample. This may be due to their water vapour and oxygen barrier properties, affecting the microbial metabolism and the oxidative and enzymatic reactions.

Fig. 3b shows the MDA levels, expressed as mg MDA/kg sample, in the meat throughout storage, where the continuous increase of MDA levels can be observed. Nonetheless, the samples packaged with the active bilayer exhibited the lowest rate of increase in the TBARS values, indicating a retarded meat oxidation, compared to the bilayer without the RS extract and control sample. This may be attributed to the radical scavenging capacity of the extract compounds that would be released on the surface of the meat. The reduced OP values of the bilayers, enhanced by the starch layer, also contributed to their oxidation inhibition capacity (Hernández-García et al., 2022; 2022). In fact, samples packaged with the PLA-TPScf bag exhibited lower oxidation levels than the control sample. This film had similar OP values to the PLAes-TPScf film, but a lower inhibition capacity of oxidative reactions. This demonstrates the active role of the antioxidant compounds of the RS extract in meat preservation. Likewise, the light barrier capacity of the active bilayer could also provide the bags with antioxidant effect, protecting the meat against undesirable photoreactions, such as the photooxidation of lipids, vitamins, and pigments. Other studies reported that the RS extracts exhibited great antioxidant activity due to a set of several phenolic acids extracted from the lignocellulosic matrix, such as ferulic, *p*-coumaric, and protocatechuic acids (Freitas, González-Martínez, & Chiralt, 2022; Menzel et al., 2020). The antioxidant ability of phenolic acids is mainly due to the hydroxyl phenolics that act as hydrogen donors, affected by the other substituents in the aromatic ring, whose positions and number influence their antioxidant activity (Topuz & Uyar, 2020). Therefore, the incorporation of active extract, as well as the use of cellulosic fractions from RS in multilayer PLA-starch systems, showed itself to have potential application to delay the oxidation of fresh pork meat.

The microbial counts in the pork meat for TV, PB, TC, and LA bacteria are shown in Fig. 3c-f. The meat samples exhibited a continuous microbial growth throughout storage, regardless of the packaging, as also reported by other authors (Andrade et al., 2022; Kim et al., 2016).

In general, no marked differences were observed between samples packaged with different films and the control sample, despite the low OP values of the bilayers that limit the amount of oxygen available for bacteria. This suggests that at the low storage temperature, oxygen availability was not limiting for microbial growth. Nevertheless, samples packaged with the active PLAes-TPScf bilayers exhibited the lowest count values throughout storage, the differences being significant for TV counts ($p < 0.05$) from the third storage day onwards. This indicates a certain antibacterial effect of the released RS extract compounds on the meat surface. In fact, samples packed with the PLAes-TPScf film reached the TV count acceptability limit (10^6-10^7 CFU/g sample, depending on the country (Kim & Jang, 2018)), 3 days later than the other treatments (Fig. 3c). Similar effects were observed by Hernández-García et al. (2022; 2022) for pork meat packaged with starch-polyester bilayer films with ferulic, *p*-coumaric, and protocatechuic acids, which are also present in the RS extract. These authors observed a slow and limited release of the phenolic acids from the polyester layer to polar simulants, which could limit the antimicrobial action of the active compound, since the minimal inhibitory concentration of the bacteria could not be reached soon enough on the food surface.

As concerns meat colour development, all of the samples exhibited a decrease in L^* values over time, becoming darker (Fig. S2a), which could be attributed to the sample water loss that promotes the pigment concentrations and refractive index near the surface encouraginging light absorption (Hernández-García et al., 2022; 2022). This effect was slightly more pronounced for meat samples packed with the PLAes-TPScf film, which exhibited a lower water vapour barrier capacity than the PLA-TPScf film. Additionally, the potential release of coloured compounds from the extract to the meat surface could contribute to the fact that these meat samples are darker while also showed the lowest colour saturation (C_{ab}^*) at the end of storage. However, this sample also exhibited the mildest changes in the h_{ab}^* values throughout storage, suggesting the smallest changes in the oxymyoglobin related with the antioxidant effect of the extract. Due to the greater change in both the C_{ab}^* and L^* values, the samples packed with PLAes-TPScf present the highest values of the ΔE^* parameter throughout storage. Nevertheless, the active PLAes-TPScf film was effective at maintaining the global colour of the meat, whereas the non-packaged samples became more yellowy-brown, which is characteristic of myoglobin oxidation. These results coincided with the lowest degree of lipid oxidation, as deduced from the TBARS analysis. Lipid and myoglobin oxidation are linked; the oxidation of one of these leads to the formation of chemicals that promotes the oxidation of the other. Several studies reported the preservation of the fresh meat colour because of the incorporation of antioxidant compounds (Faustman et al., 2010). Thus, the starch-PLA bilayer with RS extract and CF could be applied for the purposes of meat preservation, the PLA loaded with the RS extract being the food contact layer.

4. Conclusions

The PLA-TPS bilayer films containing RS extract (into PLA) and CF (into TPS) exhibited improved functional properties for food preservation with respect to the monolayer films. TPS conferred oxygen barrier capacity to the laminates, while PLA offered a wet food contact option with water vapour barrier capacity. CF incorporation into TPS reinforced the strength of the films and improved their barrier capacity. The RS extract slightly reduced the PLA resistance and elongation at break, but improved their oxygen barrier capacity. The tensile and barrier properties of bilayer films revealed changes in the performance of each layer associated with the interlayer migration of the low molecular weight compounds present in each monolayer. The bilayers with CF in the TPS sheet exhibited the lowest values of oxygen permeability while the RS extract in the PLA sheet slightly promoted the WVP and reduced resistance and elongation at break of the bilayers.

On the basis of their low oxygen permeability, the bilayers with CF reinforced TPS and PLA with and without RS antioxidant extract were used to evaluate the preservation capacity of pork meat, using PLA as the food contact layer in thermo-sealed bags. A noticeable antioxidant capacity of the RS extract was observed in the meat samples packaged with the TPScf-PLAes bags, while the microbial counts were also reduced throughout the cold storage time. Therefore, these bilayers had great potential to extend the shelf-life of meat samples, maintaining quality parameters and safety for longer, while using fractions of the RS waste which permit its valorisation.

Funding

This work was supported by Generalitat Valenciana [grant number GrisoliaP/2019/115] and project PID2019-105207RB-I00/AEI/10.13039/501100011033. Funding for open access charge: CRUE-Universitat Politècnica de València.

CRediT authorship contribution statement

Pedro A.V. Freitas: Conceptualization, Formal analysis, Investigation, Methodology, Writing – original draft, Writing – review & editing. **Consuelo González-Martínez:** Conceptualization, Formal analysis, Investigation, Methodology, Writing – original draft, Writing – review & editing. **Amparo Chiralt:** Conceptualization, Formal analysis, Investigation, Methodology, Writing – original draft, Writing – review & editing.

Declaration of Competing Interest

The authors declare that they have no known competing financial interests or personal relationships that could have appeared to influence the work reported in this paper.

Data availability

Data will be made available on request.

Acknowledgments

P.A.V.F. is grateful to Generalitat Valenciana (Spain) for the GrisoliaP/2019/115 grant.

Appendix A. Supplementary data

Supplementary data to this article can be found online at https://doi.org/10.1016/j.foodchem.2022.134990.

References

ASTM. (2005). *E96/E96M-05. Standard Test Methods for Water Vapor Transmission of Materials* (pp. 1–11). American Society for Testing and Materials.

ASTM. (2010). D3985-05 Oxygen Gas Transmission Rate Through Plastic Film and Sheeting Using a Coulometric Sensor. Annual Book of ASTM Standards, C, 1–7. 10.1520/D3985-05.2.

ASTM. (2012). ASTM D882-12 Standard test method for tensile properties of thin plastic sheeting. American Society for Testing and Materials, 12.

Andrade, J., González-Martínez, C., & Chiralt, A. (2022). Antimicrobial PLA-PVA multilayer films containing phenolic compounds. *Food Chemistry, 375*, Article 131861. https://doi.org/10.1016/j.foodchem.2021.131861

Anukiruthika, T., Sethupathy, P., Wilson, A., Kashampur, K., Moses, J. A., & Anandharamakrishnan, C. (2020). Multilayer packaging: Advances in preparation techniques and emerging food applications. *Comprehensive Reviews in Food Science and Food Safety, 19*(3), 1156–1186. https://doi.org/10.1111/1541-4337.12556

Avérous, L., Fringant, C., & Moro, L. (2001). Plasticized starch–cellulose interactions in polysaccharide composites. *Polymer, 42*(15), 6565–6572. https://doi.org/10.1016/S0032-3861(01)00125-2

Baghi, F., Gharsallaoui, A., Dumas, E., & Ghnimi, S. (2022). Advancements in biodegradable active films for food packaging: Effects of nano/microcapsule incorporation. *Foods, 11*(5), 760. https://doi.org/10.3390/foods11050760

Brand-Williams, W., Cuvelier, M. E., & Berset, C. (1995). Use of a free radical method to evaluate antioxidant activity. LWT—Food. *Science and Technology, 28*, 25–30. https://doi.org/10.1016/S0023-6438(95)80008-5

Chawla, R., Sivakumar, S., & Kaur, H. (2021). Antimicrobial edible films in food packaging: Current scenario and recent nanotechnological advancements- a review. *Carbohydrate Polymer Technologies and Applications, 2*, Article 100024. https://doi.org/10.1016/j.carpta.2020.100024

Collazo-Bigliardi, S., Ortega-Toro, R., & Chiralt, A. (2019). Improving properties of thermoplastic starch films by incorporating active extracts and cellulose fibres isolated from rice or coffee husk. *Food Packaging and Shelf Life, 22*, Article 100383. https://doi.org/10.1016/j.fpsl.2019.100383

Danilovas, P. P., Rutkaite, R., & Zemaitaitis, A. (2014). Thermal degradation and stability of cationic starches and their complexes with iodine. *Carbohydrate Polymers, 112*, 721–728. https://doi.org/10.1016/j.carbpol.2014.06.038

Fourati, Y., Magnin, A., Putaux, J.-L., & Boufi, S. (2020). One-step processing of plasticized starch/cellulose nanofibrils nanocomposites via twin-screw extrusion of starch and cellulose fibers. *Carbohydrate Polymers, 229*, Article 115554. https://doi.org/10.1016/j.carbpol.2019.115554

Freitas, P. A. V., Arias, C. I. L. F., Torres-Giner, S., González-Martínez, C., & Chiralt, A. (2021). Valorization of rice straw into cellulose microfibers for the reinforcement of thermoplastic corn starch films. *Applied Sciences, 11*(18), 8433. https://doi.org/10.3390/app11188433

Freitas, P. A. V., González-Martínez, C., & Chiralt, A. (2020). Application of ultrasound pre-treatment for enhancing extraction of bioactive compounds from rice straw. *Foods, 9*(11), 1657. https://doi.org/10.3390/foods9111657

Freitas, P. A. V., González-Martínez, C., & Chiralt, A. (2022). Applying ultrasound-assisted processing to obtain cellulose fibres from rice straw to be used as reinforcing agents. *Innovative Food Science & Emerging Technologies, 76*, Article 102932. https://doi.org/10.1016/j.ifset.2022.102932

Freitas, P. A. V., González-Martínez, C., & Chiralt, A. (2022). Antioxidant starch composite films containing rice straw extract and cellulose fibres. *Food Chemistry, 400*, Article 134073. https://doi.org/10.1016/j.foodchem.2022.134073

Galdeano, M. C., Mali, S., Grossmann, M. V. E., Yamashita, F., & García, M. A. (2009). Effects of plasticizers on the properties of oat starch films. *Materials Science and Engineering: C, 29*(2), 532–538. https://doi.org/10.1016/j.msec.2008.09.034

Hernández-García, E., Vargas, M., & Chiralt, A. (2022). Starch-polyester bilayer films with phenolic acids for pork meat preservation. *Food Chemistry, 385*, Article 132650. https://doi.org/10.1016/j.foodchem.2022.132650

Hernández-García, E. Vargas, M., & Chiralt, A. (2022b). Biodegradable multilayer films for active food packaging, based on starch and polyesters with phenolic acids. Doctoral Thesis. Accessed September 05, 2022. <https://riunet.upv.es/bitstream/handle/10251/181473/Hernandez%20-%20Biodegradable%20multilayer%20films%20for%20active%20food%20packaging%20based%20on%20starch%20and%20polyeste....pdf?sequence=1&isAllowed=y>.

Kaiser, K., Schmid, M., & Schlummer, M. (2017). Recycling of polymer-based multilayer packaging: A review. *Recycling, 3*(1), 1. https://doi.org/10.3390/recycling3010001

Kargarzadeh, H. (2017). Starch biocomposite film reinforced by multiscale rice husk fiber. *Composites Science and Technology, 9*.

Karimi, E., Mehrabanjoubani, P., Keshavarzian, M., Oskoueian, E., Jaafar, H. Z., & Abdolzadeh, A. (2014). Identification and quantification of phenolic and flavonoid components in straw and seed husk of some rice varieties (Oryza sativa L.) and their antioxidant properties: Identification and quantification of phenolic and flavonoid. *Journal of the Science of Food and Agriculture, 94*(11), 2324–2330. https://doi.org/10.1002/jsfa.6567

Kim, H. W., Jeong, J. Y., Seol, K.-H., Seong, P.-N., & Ham, J.-S. (2016). Effects of edible films containing Procyanidin on the preservation of pork meat during chilled storage. *Korean Journal for Food Science of Animal Resources, 36*(2), 230–236. https://doi.org/10.5851/kosfa.2016.36.2.230

McHUGH, T. H., Avena-Bustillos, R., & Krochta, J. M. (1993). Hydrophilic edible films: Modified procedure for water vapor permeability and explanation of thickness effects. *Journal of Food Science, 58*(4), 899–903. https://doi.org/10.1111/j.1365-2621.1993.tb09387.x

Menzel, C., González-Martínez, C., Vilaplana, F., Diretto, G., & Chiralt, A. (2020). Incorporation of natural antioxidants from rice straw into renewable starch films. *International Journal of Biological Macromolecules, 146*, 976–986. https://doi.org/10.1016/j.ijbiomac.2019.09.222

Moreno, O., Atarés, L., Chiralt, A., Cruz-Romero, M. C., & Kerry, J. (2018). Starch-gelatin antimicrobial packaging materials to extend the shelf life of chicken breast fillets. *LWT, 97*, 483–490. https://doi.org/10.1016/j.lwt.2018.07.005

Muller, J., González-Martínez, C., & Chiralt, A. (2017). Poly(lactic) acid (PLA) and starch bilayer films, containing cinnamaldehyde, obtained by compression moulding. *European Polymer Journal, 95*, 56–70. https://doi.org/10.1016/j.eurpolymj.2017.07.019

Ordoñez, R., Atarés, L., & Chiralt, A. (2022). Effect of ferulic and cinnamic acids on the functional and antimicrobial properties in thermo-processed PLA films. *Food Packaging and Shelf Life, 33*, Article 100882.

Pacquit, A., Lau, K., Mclaughlin, H., Frisby, J., Quilty, B., & Diamond, D. (2006). Development of a volatile amine sensor for the monitoring of fish spoilage. *Talanta, 69*(2), 515–520. https://doi.org/10.1016/j.talanta.2005.10.046

Peanparkdee, M., & Iwamoto, S. (2019). Bioactive compounds from by-products of rice cultivation and rice processing: Extraction and application in the food and pharmaceutical industries. *Trends in Food Science & Technology, 86*, 109–117. https://doi.org/10.1016/j.tifs.2019.02.041

Rasheed, M., Jawaid, M., Karim, Z., & Abdullah, L. C. (2020). Morphological, Physiochemical and Thermal Properties of Microcrystalline Cellulose (MCC) Extracted from Bamboo Fiber. 15.

Rasheed, M., Jawaid, M., Parveez, B., Hussain Bhat, A., & Alamery, S. (2021). Morphology, structural, thermal, and tensile properties of bamboo microcrystalline cellulose/poly(lactic acid)/poly(butylene succinate) composites. *Polymers, 13*(3), 465. https://doi.org/10.3390/polym13030465

Siracusa, V. (2012). Food packaging permeability behaviour: A report. *International Journal of Polymer Science, 2012*, 1–11. https://doi.org/10.1155/2012/302029

Siu, G. M., & Draper, H. H. (1978). A SURVEY OF THE MALONALDEHYDE CONTENT OF RETAIL MEATS AND FISH. *Journal of Food Science, 43*(4), 1147–1149. https://doi.org/10.1111/j.1365-2621.1978.tb15256.x

Sluiter, A. (2008). Determination of structural carbohydrates and lignin in biomass: Laboratory analytical procedure (LAP) (issue date: April 2008; revision date: July 2011 (Version 07–08-2011). Technical Report, 18).

Talón, E., Trifkovic, K. T., Nedovic, V. A., Bugarski, B. M., Vargas, M., Chiralt, A., & González-Martínez, C. (2017). Antioxidant edible films based on chitosan and starch containing polyphenols from thyme extracts. *Carbohydrate Polymers, 157*, 1153–1161. https://doi.org/10.1016/j.carbpol.2016.10.080

Topuz, F., & Uyar, T. (2020). Antioxidant, antibacterial and antifungal electrospun nanofibers for food packaging applications. *Food Research International, 130*, Article 108927. https://doi.org/10.1016/j.foodres.2019.108927

Vilarinho, F., Stanzione, M., Buonocore, G. G., Barbosa-Pereira, L., Sendón, R., Vaz, M. F., & Sanches Silva, A. (2021). Green tea extract and nanocellulose embedded into polylactic acid film: Properties and efficiency on retarding the lipid oxidation of a model fatty food. *Food Packaging and Shelf Life, 27*, Article 100609. https://doi.org/10.1016/j.fpsl.2020.100609

Wang, Q., Chen, W., Zhu, W., McClements, D. J., Liu, X., & Liu, F. (2022). A review of multilayer and composite films and coatings for active biodegradable packaging. *NPJ Science of Food, 6*(1), 18. https://doi.org/10.1038/s41538-022-00132-8

Yang, W., Xie, Y., Jin, J., Liu, H., & Zhang, H. (2019). Development and application of an active plastic multilayer film by coating a Plantaricin BM-1 for chilled meat preservation. *Journal of Food Science, 84*(7), 1864–1870. https://doi.org/10.1111/1750-3841.14608